

Binary Classification from Multiple Unlabeled Datasets via Surrogate Set Classification

Shida Lei^{*1} Nan Lu^{*1,2} Gang Niu² Issei Sato^{1,2} Masashi Sugiyama^{2,1}

¹The University of Tokyo ²RIKEN

{lei@ms., lu@ms., sato@, sugi@}k.u-tokyo.ac.jp, gang.niu@riken.jp

Abstract

To cope with high annotation costs, training a classifier only from *weakly supervised data* has attracted a great deal of attention these days. Among various approaches, strengthening supervision from completely unsupervised classification is a promising direction, which typically employs *class priors* as the only supervision and trains a binary classifier from *unlabeled* (U) datasets. While existing *risk-consistent* methods are theoretically grounded with high flexibility, they can learn only from *two* U sets. In this paper, we propose a new approach for binary classification from m U-sets for $m \geq 2$. Our key idea is to consider an auxiliary classification task called *surrogate set classification* (SSC), which is aimed at predicting from which U set each observed sample is drawn. SSC can be solved by a standard (multi-class) classification method, and we use the SSC solution to obtain the final binary classifier through a certain linear-fractional transformation. We built our method in a flexible and efficient *end-to-end* deep learning framework and prove it to be *classifier-consistent*. Through experiments, we demonstrate the superiority of our proposed method over state-of-the-art methods.

1 Introduction

Deep learning with large-scale supervised training data has shown great success on various tasks (Goodfellow et al., 2016). However, in practice, obtaining *strong supervision*, e.g., the complete ground-truth labels, for big data is very costly due to the expensive and time-consuming manual annotations. Thus, it is desirable for machine learning techniques to work with *weaker forms of supervision*, such as noisy labels (Natarajan et al., 2013; Liu and Tao, 2016; Patrini et al., 2017), complementary labels (Ishida et al., 2017, 2019; Feng et al., 2020), and pairwise comparison (Bao et al., 2018; Xu et al., 2019).

^{*}Equal contribution.

This paper focuses on a challenging setting which we call the U^m classification problem: our goal is to learn a binary classifier from m ($m \geq 2$) U-sets with different *class priors*, i.e., proportions of the positive data in each U set. Such a learning scenario can be conceivable in many real-world problems. For example, in computer-aided diagnosis for a certain disease (Li and Zhou, 2007), individuals' diagnosed labels may not be revealed due to privacy reasons, but unlabeled examples can be collected from a wide variety of sources, e.g., multiple hospitals. The corresponding class priors, i.e., morbidity rates in this hospital example, of each unlabeled dataset can be accessed by related medical reports and are the unique supervisions that will be leveraged throughout this work.

U^m classification is closely related to *learning with label proportions* (LLP), with a subtle difference in the experimental design.¹ Traditional LLP methods have been extensively studied in non-deep learning with strong restrictions on the model class and optimization (Quadrianto et al., 2009; Patrini et al., 2014; Yu et al., 2013). Recent methods based on *empirical proportion risk* minimization (Yu et al., 2014), i.e., minimizing the discrepancy between observed and predicted proportions, have been shown to work well in deep learning, but lack theoretical guarantees (Tsai and Lin, 2020).

Breakthroughs in U^m classification research were brought by Menon et al. (2015) and Lu et al. (2019) in proposing the *risk-consistent* methods given two U sets. Recently, Scott and Zhang (2020) extended them to incorporate multiple U sets by two steps: first, pair all the U sets so that they are sufficiently different in each pair; second, linearly combine the unbiased balanced risk estimators of all the pairs. Although this method is advantageous since it is compatible with any model architecture and stochastic optimizer, and is statistically consistent, there are several issues that limit its potential for practical use: first, the computational complexity for the optimum pairing strategy is $O(m^3)$ for m sets (Edmonds and Karp, 1972), which may not work efficiently with a large number of U sets; second, the optimal combination weights are proved based on strong model assumptions and thus remaining difficult to be tuned in practice.

Now, the question arises: can we propose computationally efficient and practical methods for U^m classification with both *flexibility* on the choice of models and optimizers and *theoretical guarantees*? The answer is affirmative.

In this paper, we provide a new approach for U^m classification by a Surrogate Set Classification task (U^m -SSC), framing the original binary classification problem into a surrogate multi-class classification task. More specifically, we regard the index of U sets as a surrogate set label and consider the supervised multi-class classification task of predicting the surrogate set label given observations. Then we theoretically bridge the original and surrogate class-posterior probabilities with a linear-fractional transformation and implement it by adding a transition layer to the neural network model. Our proposed U^m -SSC scheme is built within an end-to-end framework, which is computationally efficient, model-independent (ranging from linear to deep models), compatible with stochastic optimization, and naturally incorporates multiple U sets. Our contributions can be summarized as follows:

- Theoretically, we show that the proposed U^m -SSC method is *classifier-consistent*, i.e., the

¹The majority of LLP papers use uniform sampling for bag generation, which may result in the same proportion for all the U sets and make the LLP problem computationally intractable (Scott and Zhang, 2020). The experimental design of U^m classification described in Sec. 4 overcomes this issue.

classifier learned by the surrogate set classification task from only U data converges to the Bayes optimal classifier. Based on this, we establish an *estimation error bound* for our method.

- Practically, we propose a flexible, easy-to-implement, and computationally efficient method for the U^m classification problem, which is shown to outperform the state-of-the-art methods in most cases. We further verify the robustness of our proposed method by simulating U^m classification in the wild, e.g., on varied set sizes, extreme set numbers, inaccurate class priors, and the results are promising.

2 Problem Setup and Related Work

In this section, we introduce some notations, formulate the U^m classification problem, and review the related work.

2.1 Learning from Fully Labeled Data

Let \mathcal{X} be the input feature space and $\mathcal{Y} = \{+1, -1\}$ be a binary label space, $\mathbf{x} \in \mathcal{X}$ and $y \in \mathcal{Y}$ be the input and output random variables following an underlying joint distribution \mathcal{D} . Let $f : \mathcal{X} \rightarrow \mathbb{R}$ be an arbitrary binary classifier, and $\ell_b(t, y) : \mathbb{R} \times \mathcal{Y} \rightarrow \mathbb{R}_+$ be the *loss function* such that the value $\ell_b(t, y)$ means the loss by predicting t when the ground truth is y . The goal of binary classification is to train a classifier f that minimizes the *risk* defined as

$$R(f) = \mathbb{E}_{(\mathbf{x}, y) \sim \mathcal{D}} [\ell_b(f(\mathbf{x}), y)], \quad (1)$$

where $\mathbb{E}_{(\mathbf{x}, y) \sim \mathcal{D}}$ denotes the expectation over \mathcal{D} . For evaluation, ℓ_b is chosen as $\ell_{01}(t, y) = (1 - \text{sign}((t - \frac{1}{2}) \cdot y))/2$ and then the risk R becomes a standard performance measure in classification, a.k.a. the *classification error*. For training, ℓ_{01} is replaced by the *surrogate loss*² such as the logistic loss, since ℓ_{01} is discontinuous and therefore difficult to optimize (Ben-David et al., 2003; Bartlett et al., 2006).

In most cases, R cannot be calculated directly because the joint distribution \mathcal{D} is unknown to the learner. Given the labeled training set $\mathcal{X} = \{(\mathbf{x}_i, y_i)\}_{i=1}^n \stackrel{\text{i.i.d.}}{\sim} \mathcal{D}$ with n samples, *empirical risk minimization* (ERM) (Vapnik, 1998) is a common practice that computes an approximation of R by

$$\hat{R}(f) = \frac{1}{n} \sum_{i=1}^n \ell_b(f(\mathbf{x}_i), y_i). \quad (2)$$

2.2 Learning from Multiple Sets of U Data

Next, we consider U^m classification. We are given $m (m \geq 2)$ sets of unlabeled samples drawn from m marginal densities $\{p_{\text{tr}}^j(\mathbf{x})\}_{j=1}^m$, where:

$$p_{\text{tr}}^j(\mathbf{x}) = \pi_j p_{\text{p}}(\mathbf{x}) + (1 - \pi_j) p_{\text{n}}(\mathbf{x}), \quad (3)$$

²The surrogate loss ℓ_s should be *classification-calibrated* so that the predictions can be the same for classifiers learned using ℓ_s and ℓ_{01} (Bartlett et al., 2006).

each $p_{\text{tr}}^j(\mathbf{x})$ is seen as a mixture of the positive and negative class-conditional densities $(p_p(\mathbf{x}), p_n(\mathbf{x})) = (p(\mathbf{x}|y=+1), p(\mathbf{x}|y=-1))$, and $\pi_j = p_{\text{tr}}^j(y=+1)$ denotes the class prior of the j -th unlabeled set. We assume that the class priors $\{\pi_j\}_{j=1}^m$ are known, which are the only *weak supervision* we will leverage in this work. To make the problem mathematically solvable, among the m sets of U data, we assume at least two of them are different, i.e., $\exists j, j' \in \{1, \dots, m\}$ such that $j \neq j'$ and $\pi_j \neq \pi_{j'}$.

In contrast to supervised classification where we have fully labeled training set \mathcal{X} directly drawn from \mathcal{D} , we only have access to m sets of unlabeled data $\mathcal{X}_{\text{tr}} = \{\mathcal{X}_{\text{tr}}^j\}_{j=1}^m$, where:

$$\mathcal{X}_{\text{tr}}^j = \{\mathbf{x}_1^j, \dots, \mathbf{x}_{n_j}^j\} \stackrel{\text{i.i.d.}}{\sim} p_{\text{tr}}^j(\mathbf{x}), \quad (4)$$

where n_j denotes the sample size of the j -th U set. But our goal is still the same as supervised classification: to obtain a binary classifier that generalizes well with respect to \mathcal{D} , despite the fact that it is unobserved.

2.3 Related Work

Classification risk methods To solve the problem, [Lu et al. \(2019\)](#) assumed $m = 2$ and $\pi_1 > \pi_2$, and proposed an equivalent expression of the classification risk (1):

$$\begin{aligned} R_{\text{UU}}(f) &= \underbrace{\mathbb{E}_{\mathbf{x} \sim p_{\text{tr}}^1} c_1^+ \ell(f(\mathbf{x}), +1) - \mathbb{E}_{\mathbf{x} \sim p_{\text{tr}}^2} c_2^+ \ell(f(\mathbf{x}), +1)}_{R_{\text{UU-p}}(f)} \\ &\quad - \underbrace{\mathbb{E}_{\mathbf{x} \sim p_{\text{tr}}^1} c_1^- \ell(f(\mathbf{x}), -1) + \mathbb{E}_{\mathbf{x} \sim p_{\text{tr}}^2} c_2^- \ell(f(\mathbf{x}), -1)}_{R_{\text{UU-n}}(f)}, \end{aligned} \quad (5)$$

where $c_1^+ = \frac{(1-\pi_2)\pi_{\mathcal{D}}}{\pi_1-\pi_2}$, $c_1^- = \frac{\pi_2(1-\pi_{\mathcal{D}})}{\pi_1-\pi_2}$, $c_2^+ = \frac{(1-\pi_1)\pi_{\mathcal{D}}}{\pi_1-\pi_2}$, $c_2^- = \frac{\pi_1(1-\pi_{\mathcal{D}})}{\pi_1-\pi_2}$, and $\pi_{\mathcal{D}}$ denotes the class prior of the test set. If $\pi_{\mathcal{D}}$ is assumed to be $\frac{1}{2}$ in $R_{\text{UU}}(f)$, the obtained $R_{\text{UU-b}}(f)$ ([Menon et al., 2015](#)) corresponds to the balanced risk, a.k.a. the *balanced error* ([Brodersen et al., 2010](#)):

$$R_{\text{b}}(f) = \frac{1}{2} \mathbb{E}_{\mathbf{x} \sim p_p} [\ell_b(f(\mathbf{x}), +1)] + \frac{1}{2} \mathbb{E}_{\mathbf{x} \sim p_n} [\ell_b(f(\mathbf{x}), -1)]. \quad (6)$$

Note that $R_{\text{b}}(f) = R(f)$ for any f if and only if $\pi_{\mathcal{D}} = \frac{1}{2}$, which means that it definitely biases learning when $\pi_{\mathcal{D}} \approx \frac{1}{2}$ is not the case. Given $\mathcal{X}_{\text{tr}}^1$ and $\mathcal{X}_{\text{tr}}^2$, $R_{\text{UU}}(f)$ and $R_{\text{UU-b}}(f)$ can be approximated by their corresponding empirical counterparts $\hat{R}_{\text{UU}}(f)$ and $\hat{R}_{\text{UU-b}}(f)$, respectively.

Since the unbiased estimators \hat{R}_{UU} and $\hat{R}_{\text{UU-b}}$ contain some negative terms, which may incur a negative training risk and cause overfitting. More specifically, although the original risks are non-negative if the loss is non-negative, their empirical counterparts can take negative values which causes overfitting ([Lu et al., 2020](#)). So [Lu et al. \(2020\)](#) proposed a corrected learning objective that wraps empirical risks for the positive class $\hat{R}_{\text{UU-p}}(f)$ and the negative class $\hat{R}_{\text{UU-n}}(f)$ of Eq. (5) into some non-negative function f_c , such that $f_c(x) = x$ for all $x \geq 0$ and $f_c(x) > 0$ for all $x < 0$:

$$\hat{R}_{\text{UU-c}}(f) = f_c(\hat{R}_{\text{UU-p}}(f)) + f_c(\hat{R}_{\text{UU-n}}(f)). \quad (7)$$

Table 1: Comparisons of the proposed method with previous works in the U^m classification setting.
 “Class.” stands for Classification.

Methods	Deal with 2+ sets	Theoretical guarantee	Non-negative	Pre-computing complexity	Risk Measure
$\widehat{R}_{UU}(f)$ (Lu et al., 2019)	×	✓	×	$O(1)$	Class. risk (1)
$\widehat{R}_{UU-b}(f)$ (Menon et al., 2015)	×	✓	×	$O(1)$	Balanced risk (6)
$\widehat{R}_{UU-c}(f)$ (Lu et al., 2020)	×	✓	✓	$O(1)$	Class. risk (1)
$\widehat{R}_{U^m}(f)$ (Scott and Zhang, 2020)	✓	✓	×	$O(m^3)$	Balanced risk (6)
$\widehat{R}_{Prop}(f)$ (Tsai and Lin, 2020)	✓	✗	✓	$O(1)$	Proportion risk (9)
Proposed	✓	✓	✓	$O(1)$	Class. risk (1)

Note that \widehat{R}_{UU-c} is biased with finite samples, but Lu et al. (2020) showed its risk-consistency, i.e., it converges to true R if $n_1, n_2 \rightarrow \infty$.

Though these risk-consistent methods are advantageous (e.g., model-independent and theoretically guaranteed), they are limited to 2 U sets. Scott and Zhang (2020) extended the previous method for the general $m (m \geq 2)$ setting. More specifically, they assumed the number of sets $m = 2k$ and proposed a pre-processing step that finds k pairs of the U sets by solving a maximum weighted matching problem (Edmonds, 1965). Then they linearly combine the unbiased balanced risk estimator of each pair³. The resulted weighted learning objective is given by

$$\widehat{R}_{U^m}(f) = \sum_{j=1}^k \omega_j \widehat{R}_{UU-b}(f). \quad (8)$$

This method is promising but has some practical issues: the pairing step is computationally very inefficient and the weights are hard to tune in practice.

Proportion risk methods Another line of research on U^m classification studied the *empirical proportion risk* (EPR) that is defined as

$$\widehat{R}_{Prop}(f) = \sum_{j=1}^m d_{prop}(\pi_j, \hat{\pi}_j), \quad (9)$$

where π_j and $\hat{\pi}_j = \frac{1}{n_j} \sum_{i=1}^{n_j} \frac{1+\text{sign}(f(\mathbf{x}_i^j)-1/2)}{2}$ are the true and predicted label proportions for j -th U set \mathcal{X}_{tr}^j , and d_{prop} is a distance function (Yu et al., 2014).

The state-of-the-art method in this line (Tsai and Lin, 2020) combined EPR with the consistency regularization and proposed the following learning objective:

$$\widehat{R}_{Prop-c}(f) = \widehat{R}_{Prop}(f) + \alpha \ell_{cons}(f), \quad (10)$$

where $\ell_{cons}(f) = d_{cons}(f(\mathbf{x}), f(\hat{\mathbf{x}}))$ is the consistency loss given a distance function d_{cons} and $\hat{\mathbf{x}}$ is a perturbed input from the original one \mathbf{x} .

A comparison of the previous works with our proposed method that will be introduced in Sec. 3 is given in Table 1.

³In Scott and Zhang (2020), it is assumed that $\pi_1 \neq \pi_2$ in each pair, which is a stronger assumption than ours.

3 U^m classification via Surrogate Set Classification

In this section, we present a new method for learning from multiple U sets via a surrogate set classification task. We first introduce the surrogate task, theoretically bridging the surrogate and original class probabilities, and then provide our algorithm with a neural network. Finally, we provide theoretical guarantees for the proposed method.

3.1 Surrogate Set Classification Task

The main challenge in the U^m classification problem is that we have *no* access to the ground-truth labels of the training examples so that the empirical risk for supervised binary classification (2) cannot be directly computed. Our idea is to consider a surrogate set classification task that could be tackled easily from the given unlabeled datasets instead. This serves as a proxy and gives us a *classifier-consistent* solution to the original binary classification problem.

Specifically, denote by $\bar{y} \in \{1, 2, \dots, m\}$ the index of the U set, equivalently, the index of the corresponding marginal density. By treating \bar{y} as the *surrogate label*, we formulate the surrogate set classification task as a standard multi-class classification. Let $\bar{\mathcal{D}}$ be the joint distribution for the random variables $\mathbf{x} \in \mathcal{X}$ and $\bar{y} \in \{1, 2, \dots, m\}$. Any $\bar{\mathcal{D}}$ could be identified via the class priors $\{\rho_j\}_{j=1}^m$ and class-conditional densities $\{p(\mathbf{x} \mid \bar{y} = j)\}_{j=1}^m$, where ρ_j can be estimated by $\rho_j = \frac{n_j}{\sum_{j=1}^m n_j}$ and $p(\mathbf{x} \mid \bar{y} = j) = p_{\text{tr}}^j(\mathbf{x})$.

Our goal is to train a classifier $\mathbf{g}(\mathbf{x}) : \mathcal{X} \rightarrow \mathbb{R}^m$ that minimizes the following risk:

$$R_{\text{Surr}}(\mathbf{g}) = \mathbb{E}_{(\mathbf{x}, \bar{y}) \sim \bar{\mathcal{D}}} [\ell(\mathbf{g}(\mathbf{x}), \bar{y})], \quad (11)$$

where $\ell(\mathbf{g}(\mathbf{x}), \bar{y}) : \mathbb{R}^m \times \bar{\mathcal{Y}} \rightarrow \mathbb{R}_+$ is a proper loss for m -class classification, e.g., the *cross-entropy loss*:

$$\ell_{\text{ce}}(\mathbf{g}(\mathbf{x}), \bar{y}) = - \sum_{j=1}^m \mathbf{1}(\bar{y} = j) \log(g_j(\mathbf{x})) = - \log(g_{\bar{y}}(\mathbf{x})),$$

where $\mathbf{1}(\cdot)$ is the indicator function. Typically, the predicted label \bar{y}_{pred} takes the form $\bar{y}_{\text{pred}} = \text{argmax}_{j \in m} g_j(\mathbf{x})$, where $g_j(\mathbf{x})$ is the j -th element of $\mathbf{g}(\mathbf{x})$, and is a score function that estimates the true class-posterior probability $\bar{\eta}_j(\mathbf{x}) = p(\bar{y} = j \mid \mathbf{x})$.

Now the unlabeled training sets \mathcal{X}_{tr} defined in Eq. (4) for the binary classification can be seen as a labeled training set $\mathcal{X}_{\text{tr}} = \{(\mathbf{x}_i, \bar{y}_i)\}_{i=1}^{n_{\text{tr}}} \stackrel{\text{i.i.d.}}{\sim} \bar{\mathcal{D}}$ for the multi-class classification, where n_{tr} is the total number of U data. We can use them to approximate the risk R_{Surr} by

$$\hat{R}_{\text{Surr}}(\mathbf{g}) = \frac{1}{n_{\text{tr}}} \sum_{i=1}^{n_{\text{tr}}} \ell(\mathbf{g}(\mathbf{x}_i), \bar{y}_i). \quad (12)$$

3.2 Bridging Two Posterior Probabilities

Let $\eta(\mathbf{x}) = p(y = +1 \mid \mathbf{x})$ be the class-posterior probability for class $+1$ in the original binary classification problem, and $\bar{\eta}_j(\mathbf{x}) = p(\bar{y} = j \mid \mathbf{x})$ be the class-posterior probability for class j in the surrogate set classification problem. We theoretically bridge them by the following theorem.

Theorem 1. *By the definitions of \mathcal{D} , $\eta(\mathbf{x})$, $\bar{\mathcal{D}}$, and $\bar{\eta}_j(\mathbf{x})$, we have*

$$\bar{\eta}_j(\mathbf{x}) = Q_j(\eta(\mathbf{x})), \quad \forall j = 1, \dots, m, \quad (13)$$

where

$$Q_j(\eta(\mathbf{x})) = \frac{a_j \cdot \eta(\mathbf{x}) + b_j}{c \cdot \eta(\mathbf{x}) + d},$$

$$a_j = \rho_j(\pi_j - \pi_{\mathcal{D}}), \quad b_j = \rho_j \pi_{\mathcal{D}}(1 - \pi_j), \quad c = \sum_{j=1}^m \rho_j(\pi_j - \pi_{\mathcal{D}}), \quad \text{and} \quad d = \sum_{j=1}^m \rho_j \pi_{\mathcal{D}}(1 - \pi_j).$$

Such a relationship has been previously studied by [Menon et al. \(2015\)](#) in the context of *corrupted label learning* for a specific 2×2 case, i.e., 2 clean classes are transformed to 2 corrupted classes, and they used the relationship to post-processing the threshold of the score function learned from corrupted data. Our proposal can be regarded as its extension to a general $2 \times m$ case and is used to connect a binary-label-class classifier with a multi-set-class classifier.

Let $\mathbf{Q}(\cdot) : \mathbb{R} \rightarrow \mathbb{R}^m$ be the vector form of functions $\mathbf{Q}(\cdot) = [Q_1(\cdot), \dots, Q_m(\cdot)]^\top$. Note that the coefficients in $Q_i(\cdot)$ are all constants and $\mathbf{Q}(\cdot)$ is deterministic. We further study good properties of the transformation function \mathbf{Q} in the following lemma, which implies the feasibility of approaching $\eta(\mathbf{x})$ by means of estimating $\bar{\eta}_j(\mathbf{x})$.

Lemma 2. *The transformation $\mathbf{Q}(\cdot)$ given in Theorem 1 is an injective function in the domain $[0, 1]$.*

3.3 Classifier-consistent Algorithm

Given the transformation function \mathbf{Q} , we have two approaches to obtain $\eta(\mathbf{x})$ from $\bar{\eta}_j(\mathbf{x})$. First, one can estimate $\bar{\eta}_j(\mathbf{x})$, then calculate $\eta(\mathbf{x})$ via the inverse function $Q_j^{-1}(\bar{\eta}_j(\mathbf{x}))$. Second, one can encode $\eta(\mathbf{x})$ as a latent variable into the computation of $\bar{\eta}_j(\mathbf{x})$ and obtain both of them simultaneously. We prefer the latter for three reasons:

- Computational efficiency. The latter provides a one-step solution and avoids an additional computation of the inverse functions, which provides computational efficiency and easiness for the implementation.
- Robustness. Since the coefficients of $Q_j(\cdot)$ could be disturbed by noise in practice, its inversion in the former solution may enlarge the noise by orders of magnitude, which makes the learning less robust.
- Identifiability. Calculating $Q_j^{-1}(\bar{\eta}_j(\mathbf{x}))$ for all $j = \{1, \dots, m\}$ induces m estimations of $\eta(\mathbf{x})$ and they are usually non-identical, due to the estimation error of $\bar{\eta}_j(\mathbf{x})$ from finite training samples or noisy $Q_j(\cdot)$, which introduces a new problem to solve this conflict.

Therefore, we embed the estimation of $\eta(\mathbf{x})$ into the estimation of $\bar{\eta}_j(\mathbf{x})$: let $f(\mathbf{x})$ be the model output that estimates $\eta(\mathbf{x})$, then we make use of transition functions $\mathbf{Q}(\cdot)$ and model $g_j(\mathbf{x}) = Q_j(f(\mathbf{x}))$. Based on this, we propose to learn with the following modified loss function:

$$\ell(\mathbf{g}(\mathbf{x}), \bar{y}) = \ell(\mathbf{Q}(f(\mathbf{x})), \bar{y}), \quad (14)$$

Algorithm 1 U^m -SSC

Input: Model f , m sets of unlabeled data \mathcal{X}_{tr} , class priors π_j and $\pi_{\mathcal{D}}$

- 1: Compute coefficients a_j , b_j , c and d of $\mathbf{Q}(\cdot)$ in Theorem 1 using π_j and $\pi_{\mathcal{D}}$.
- 2: Let $\mathbf{g} = \mathbf{Q}(f)$ and \mathcal{A} be an SGD-like optimizer working on \mathbf{g} .
- 3: **for** $t = 1, 2, \dots, \text{number_of_epochs}$ **do**
- 4: Shuffle \mathcal{X}_{tr}
- 5: **for** $i = 1, 2, \dots, \text{number_of_mini-batches}$ **do**
- 6: Fetch mini-batch $\bar{\mathcal{X}}_{\text{tr}}$ from \mathcal{X}_{tr}
- 7: Forward $\bar{\mathcal{X}}_{\text{tr}}$ and get $f(\bar{\mathcal{X}}_{\text{tr}})$
- 8: Compute $\mathbf{g}(\bar{\mathcal{X}}_{\text{tr}}) = \mathbf{Q}(f(\bar{\mathcal{X}}_{\text{tr}}))$
- 9: Compute loss from Eq.(12) using $\mathbf{g}(\bar{\mathcal{X}}_{\text{tr}})$
- 10: Update \mathbf{g} by \mathcal{A} , which induces an update on f
- 11: **end for**
- 12: **end for**

Output: f

where $\mathbf{Q}(f(\mathbf{x})) = [Q_1(f(\mathbf{x})), \dots, Q_m(f(\mathbf{x}))]^{\top}$. The corresponding expected loss for the surrogate task can be written as

$$\begin{aligned} R_{\text{Surr}}(f) &= \mathbb{E}_{(\mathbf{x}, \bar{y}) \sim \bar{\mathcal{D}}} [\ell(\mathbf{Q}(f(\mathbf{x})), \bar{y})] \\ &= \mathbb{E}_{(\mathbf{x}, \bar{y}) \sim \bar{\mathcal{D}}} [\ell(\mathbf{g}(\mathbf{x}), \bar{y})] = R_{\text{Surr}}(\mathbf{g}). \end{aligned} \quad (15)$$

So an equivalent expression of the learning objective (12) is given by

$$\widehat{R}_{\text{Surr}}(f) = \frac{1}{n_{\text{tr}}} \sum_{i=1}^{n_{\text{tr}}} \ell(\mathbf{Q}(f(\mathbf{x}_i)), \bar{y}_i). \quad (16)$$

In order to prove that this method is classifier-consistent, we introduce the following lemma.

Lemma 3. *Provided that a certain loss function, e.g., the softmax cross-entropy or mean squared error, is chosen for ℓ , we have the optimum mapping \mathbf{g}^* for $R_{\text{Surr}}(\mathbf{g}; \ell)$ in (11) satisfies $\mathbf{g}^* = \bar{\eta}$.*

Lemma 3 ensures that $\mathbf{g}^* = \operatorname{argmin}_{\mathbf{g}} R_{\text{Surr}}(\mathbf{g}; \ell) = \bar{\eta}$ under mild conditions, and it is satisfied for all $m \geq 2$. Since $\mathbf{g}(\mathbf{x}) = \mathbf{Q}(f(\mathbf{x}))$ and $\mathbf{Q}(\cdot)$ is deterministic, when considering minimizing $R_{\text{Surr}}(f)$ that takes f as the argument, we have the following theorem.

Theorem 4 (Identification of the optimal binary classifier). *Assume that the cross-entropy loss or mean squared error is used for ℓ and ℓ_b . Let f_{Surr}^* be the U^m -SSC optimal classifier induced by \mathbf{g}^* , and f^* be the minimizer of $R(f)$ in (1). Then we have $f_{\text{Surr}}^* = f^*$.*

So far, we have proved that U^m -SSC is a classifier-consistent algorithm. Given an enough number of samples, the optimal classifier for the original binary classification task can be identified. We provide the U^m -SSC algorithm in Algorithm 1 and illustrate the implementation in Fig. 1.

We implement the transition function $\mathbf{Q}(\cdot)$ by adding a transition layer following the sigmoid function of the neural network (NN). At the training phase, a sample $(\mathbf{x}_{\text{tr}}, \bar{y}_{\text{tr}})$ is fetched to the

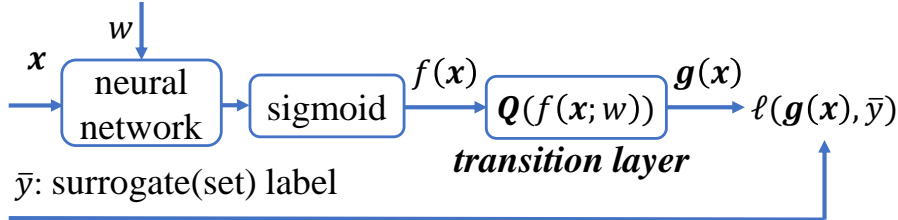


Figure 1: Illustration of the implementation of U^m -SSC.

network. A sigmoid function $f_{\text{sig}}(x) = \frac{1}{1+e^{-x}}$ is used to map the output of NN to the range $[0, 1]$ such that the output $f(\mathbf{x})$ is an estimate of the class-posterior probability $\eta(\mathbf{x})$. Then $f(\mathbf{x})$ is forwarded to the transition layer and a vector output $\mathbf{g}(\mathbf{x}) = \mathbf{Q}(f(\mathbf{x}))$ is computed. The loss computed on the output $\mathbf{g}(\mathbf{x})$ and surrogate label \bar{y}_{tr} in Eq. (12) is then used for updating the NN weights. Note that the transition layer is fixed and only weights in the base network are learnable. At the test phase, for any test sample \mathbf{x}_{te} , we compute $f(\mathbf{x}_{\text{te}})$ using only the trained base network and sigmoid function. The test sample is classified by using the sign function as $\text{sign}(f(\mathbf{x}_{\text{te}}) - \frac{1}{2})$. Our method is model-agnostic and can be easily trained with a stochastic optimization algorithm, which ensures its scalability to large-scale datasets.

3.4 Theoretical Analysis

In what follows, we establish an upper bound for the estimation error of our method. This upper bound also illustrates the convergence rate of the classifier learned from m U sets to the Bayes optimal classifier. Let \hat{f}_{Surr} be the optimum solution obtained by minimizing $\hat{R}_{\text{Surr}}(f)$. We will upper-bound the difference between \hat{f}_{Surr} and f^* by upper-bounding $R_{\text{Surr}}(\hat{f}_{\text{Surr}}) - R_{\text{Surr}}(f^*)$.

In order to derive a bound for the Rademacher complexity $\mathfrak{R}_n(\ell \circ \mathcal{F})$, we investigate the Lipschitz continuity of loss function $\ell(\mathbf{Q}(f(\mathbf{x})), \bar{y})$ and introduce the following lemma,

Lemma 5. *Suppose that among all class priors of U sets, there are at least two of them which are different, i.e., $\exists j \in \{1, \dots, m\}, j' \in \{1, \dots, m\}$ such that $j \neq j'$ and $\pi_j \neq \pi_{j'}$. Assume $0 < f(\mathbf{x}) < 1, \forall \mathbf{x} \in \mathcal{X}$, e.g., $f(\mathbf{x})$ is mapped to $[0, 1]$ by the sigmoid activation function. Then, $\forall j = 1, \dots, m$, the function $Q_j(f(\mathbf{x}))$ is Lipschitz continuous w.r.t. $f(\mathbf{x})$ with a Lipschitz constant $2/\alpha^2$, where*

$$\alpha = \min \left(\sum_{j=1}^m \rho_j \pi_j (1 - \pi_j), \sum_{j=1}^m \rho_j \pi_j (1 - \pi_j) \right).$$

Then, we have the following conclusion on the estimation error.

Theorem 6 (Estimation error bound). *Assume $\ell(\mathbf{Q}(f), \bar{y})$ is upper-bounded by M_ℓ and is \mathcal{L}_ℓ -Lipschitz continuous w.r.t. $\mathbf{Q}(f)$. Define the Rademacher complexity $\mathfrak{R}_{n_j}(\mathcal{F}) = \mathbb{E}[\sup_{f \in \mathcal{F}} \frac{1}{n_j} \sum_{i=1}^{n_j} \sigma_i f(\mathbf{x}_i)] \forall j = 1, \dots, m$, where $\mathcal{F} = \{f : \mathcal{X} \rightarrow \mathbb{R}\}$ is a class of measurable functions and $\{\sigma_1, \dots, \sigma_{n_j}\}$ are Rademacher variables uniform randomly taking values from*

Table 2: Specification of datasets and corresponding models

Dataset	# Train	# Test	# Features	$\pi_{\mathcal{D}}$	Model
MNIST	60,000	10,000	784	0.49	5-layer MLP
Fashion-MNIST	60,000	10,000	784	0.8	5-layer MLP
Kuzushiji-MNIST	60,000	10,000	784	0.3	5-layer MLP
CIFAR-10	50,000	10,000	3,072	0.7	ResNet-32

$\{-1, +1\}$. Then, with probability at least $1 - \delta$, we have

$$\begin{aligned}
R_{\text{Surr}}(\hat{f}_{\text{Surr}}) - R_{\text{Surr}}(f^*) &\leq \\
\frac{4\sqrt{2}\mathcal{L}_\ell}{\alpha^2} \sum_{j=1}^m \mathfrak{R}_{n_j}(\mathcal{F}) + M_\ell \sqrt{\frac{\log(1/\delta)}{2n_{\text{tr}}}}.
\end{aligned} \tag{17}$$

Theorem 6 demonstrates that as the number of training samples goes to infinity, the risk of \hat{f}_{Surr} converges to the risk of f^* . Moreover, the coefficient α implies that a tighter error bound could be obtained when the class priors π_j are close to 0 or 1. This conclusion agrees with our intuition that purer U sets (contains almost only positive/ negative instances) lead to better performance.

4 Experiments

In this section, we experimentally analyze the proposed method and compare it with state-of-the-art methods in the U^m classification setting.

Datasets We train on widely adopted benchmarks MNIST (LeCun et al., 1998), Fashion-MNIST (Xiao et al., 2017), Kuzushiji-MNIST (Clanuwat et al., 2018) and CIFAR-10 (Krizhevsky, 2009). Since all four datasets contain 10 classes originally, we manually corrupt them into binary classification datasets. More details about the experimental setup can be found in Appendix B. Table 2 briefly summarizes the benchmark datasets.

We generate m sets of U training data according to Eq. (4). For each dataset, the total number of training samples T is fixed, the number of instances contained in each set is also fixed as T/m . In order to simulate the real-world cases, we uniformly sample the class priors π_j from range $[0.1, 0.9]$ for all U sets. We checked that the generated class priors are not all identical, which is often the case, to make sure the problem is mathematically solvable. Notice that the class priors are determined before sampling and are not all equal in our setup, which is essentially different from the uniform set generation setup used in most LLP literature.

Baselines In order to better analyze the performance of the proposed method, we compare it with state-of-the-art methods based on the classification risk (Scott and Zhang, 2020) and the empirical proportion risk (Tsai and Lin, 2020) for the U^m classification problem. Recall that the proposed

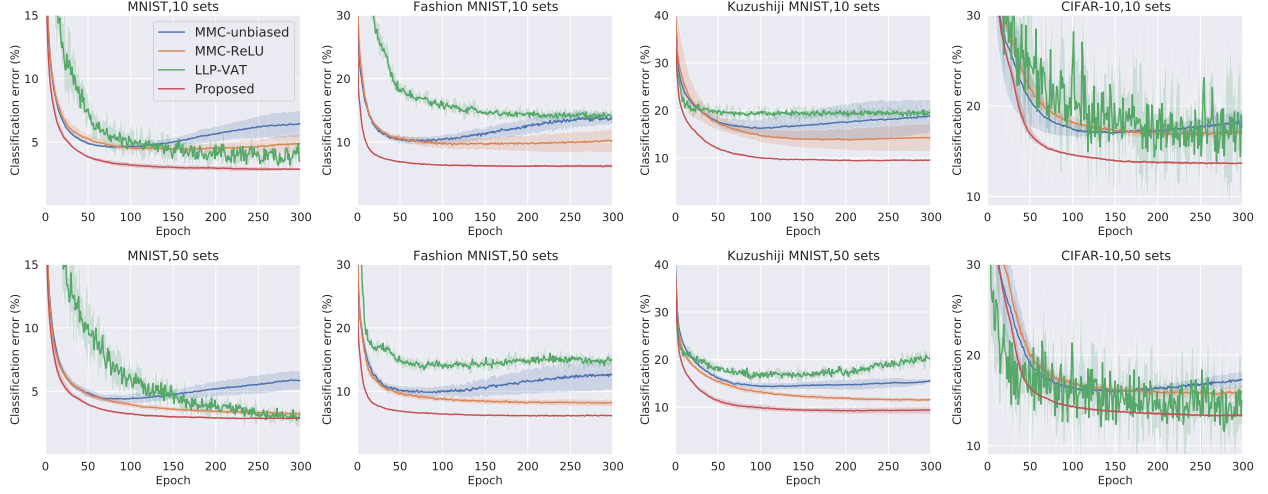


Figure 2: Experimental results of learning from 10 and 50 sets of U data.

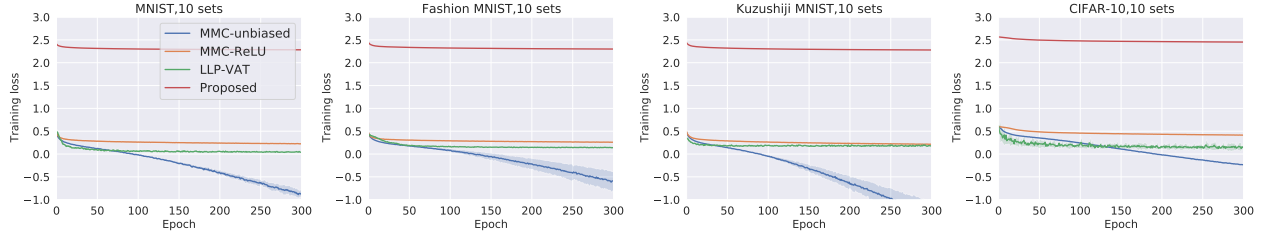


Figure 3: Training loss of learning from 10 sets of U data.

learning objective $\widehat{R}_{U^m}(f)$ (8) in [Scott and Zhang \(2020\)](#) is a combination of unbiased balanced risk estimators $\widehat{R}_{UU-b}(f)$, which are observed to have an overfitting issue due to the negative empirical risks by [Lu et al. \(2020\)](#). We observe the same issue for the combined learning objective $\widehat{R}_{U^m}(f)$ (see Sec 4.2 for more details), so we make a non-negative correction for $\widehat{R}_{UU-b}(f)$ according to the proposed method in [\(Lu et al., 2020\)](#) and produce a stronger baseline. The baselines are summarized as follows:

- MMC-unbiased: the multiple mutual contamination MMC framework based method $\widehat{R}_{U^m}(f)$ proposed by [Scott and Zhang \(2020\)](#);
- MMC-ReLU: the $\widehat{R}_{U^m}(f)$ method with a non-negative correction [\(Lu et al., 2020\)](#) by the rectified linear unit (ReLU) function;
- LLP-VAT: the empirical proportion risk framework based method proposed by [Tsai and Lin \(2020\)](#).

Experimental setup The models are optimizers used are also described in Table 2. In the table, MLP refers to *multi-layer perceptron*, ResNet refers to *residual networks* ([He et al., 2016](#)) and their detailed architectures are in Appendix B. As a common practice, we use Adam ([Kingma and Ba, 2015](#)) with cross-entropy loss for optimization. We train 300 epochs for all the experiments, and the classification error rate is evaluated for performance at testing. Note that for a fair comparison, we use the same models and hyper-parameters for the implementation of all methods. All the

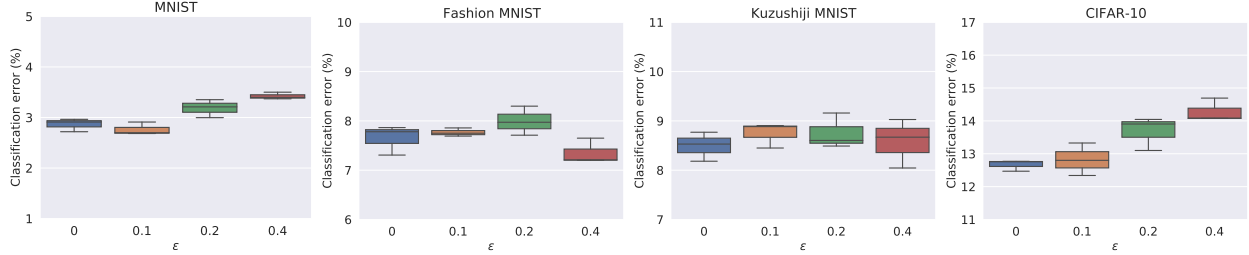


Figure 4: Box plot of the test errors for the proposed U^m -SSC method tested on learning from 50 U sets with inaccurate class priors ($\epsilon = 0$ means *true*; larger ϵ , larger noise).

experiments are repeated 3 times and the mean error with standard deviation is recorded for each method.

4.1 Comparison with State-of-the-art Methods

We first compare our proposed method with state-of-the-art methods for U^m classification. The experimental results on learning from 10 and 50 U sets are reported in Fig. 2, and the table of final errors can be found in Appendix C.

We can see that the *classification risk* (CR) based methods, i.e., MMC-unbiased, MMC-ReLU and our proposed U^m -SSC generally outperform the *empirical proportion risk* (EPR) based method, i.e., LLP-VAT, with lower classification error and more stability, which demonstrates the superiority of the *consistent* methods. Within the CR based methods, the proposed U^m -SSC method significantly outperforms the MMC methods when $\pi_{\mathcal{D}} \approx \frac{1}{2}$ is not true, which corresponds to our analysis that the balanced classification risk (6) is biased and thus the performance of MMC-based methods degrades. This observed trend emphasizes again our advantage of using classification error as the objective. When $\pi_{\mathcal{D}} \approx \frac{1}{2}$ is true, i.e., for the MNIST dataset, the U^m -SSC method still outperforms the MMC methods, and we argue that this advantage comes from the surrogate set classification mechanism in U^m -SSC, which implies the classifier-consistent methods perform better than the risk-consistent methods.

Also note that our method is fairly stable w.r.t. set numbers m , including extremely large ($m = 100, 500, 1000$) or small ($m = 2$) values (see additional experiments in Appendix C.4).

4.2 On the Training Loss

In this experiment, we are interested in the characteristics of the training losses of all methods and analyze them in Fig. 3. Our observations are as follows. First, we confirm that the empirical risk of the MMC-unbiased method goes negative during training, which incurs overfitting as shown in Fig. 2. Other methods do not have this negative empirical risk issue. And we can see that the improved MMC-ReLU method effectively mitigates this overfitting. The results are consistent with the observations in Lu et al. (2020). Second, we notice that the training loss of the proposed U^m -SSC is obviously higher than all other baseline methods. This is due to the added adaptation layer that shrinks the output range. We provide a detailed analysis in Appendix C.2. A notable effect is that our method is suitable for a relatively small learning rate.

Table 3: Mean errors (standard deviations) over three trials in percentage for the proposed U^m -SSC method tested on different set sizes. The uniform set size n_u is shifted to $\delta \cdot n_u$ (smaller δ , larger shift). Random means uniformly sample a set size from range $[0, T]$.

Dataset	Sets	n_u	$\delta = 0.8$	$\delta = 0.6$	$\delta = 0.4$	$\delta = 0.2$	Random
MNIST	10	6000	2.83 (0.18)	2.91 (0.04)	3.2 (0.2)	3.19 (0.35)	2.66 (0.08)
	50	1200	2.46 (0.1)	2.58 (0.08)	2.76 (0.13)	2.97 (0.11)	3.0 (0.12)
Fashion -MNIST	10	6000	7.88 (0.21)	7.68 (0.36)	7.84 (0.17)	7.89 (0.24)	7.04 (0.13)
	50	1200	8.29 (0.19)	8.91 (0.29)	7.61 (0.55)	8.8 (0.31)	8.62 (0.24)
Kuzushiji -MNIST	10	6000	8.98 (0.52)	9.83 (0.57)	9.43 (0.41)	10.03 (0.81)	8.38 (0.31)
	50	1200	9.35 (0.33)	9.53 (0.64)	9.89 (0.72)	11.08 (0.61)	10.34 (0.73)
CIFAR- 10	10	5000	12.55 (0.61)	12.25 (0.8)	12.41 (0.35)	12.49 (0.98)	11.65 (0.44)
	50	1000	12.16 (0.23)	12.19 (0.75)	12.88 (0.37)	13.66 (0.54)	12.09 (0.42)

4.3 On the Variation of Set Size

The set size may vary from a large range depends on different tasks in the real world. However, as the set size shifts, given our data generation process in (3), the marginal distribution of the training data $p(\mathbf{x})$ shifts from that of the test one, which causes the *covariate shift*. To verify the robustness of our proposed method against the shift, we conducted experiments on the variation of set size. We investigate two kinds of set size shift:

- Based on the uniform set size, all sets contain T/m U data. We fix the sizes of half U sets and change the sizes of the other half to $\delta \cdot T/m$ where $\delta \in [0, 1]$.
- Uniformly sample set size for each U set from range $[0, T]$ such that $\sum_{j=1}^m n_j = T$.

As shown in Table 3, the proposed method is reasonably robust as δ moves to 0. The slight degradation may come from the decreased total number of training samples T as δ decreases. We also find that the random set size setting reaches the best performance in 3 out of 4 datasets. Since this is a more natural way for size generation, the robustness of the proposed method on varied set size can be verified.

4.4 Robustness against Inaccurate Class Priors

Hitherto, we have assumed that the values of class priors π_j are accessible and accurately used in model construction, which may not be true in practice. In order to simulate the U^m classification setting in the wild, where we must suffer from some errors from estimating the class priors, we design experiments that add random noise to all class priors. More specifically, the U^m -SSC method is tested by replacing π_j with the noisy $\pi'_j = \gamma_j \cdot \pi_j$, where ϵ is a small number and γ_j is randomly sampled from $[1 - \epsilon, 1 + \epsilon]$, so that the method would treat noisy π'_j as the true π_j during the whole learning process. Note that we tailor the noisy π_j to $[0, 1]$ if it surpasses the range.

The results on learning from 50 sets with inaccurate class priors are reported in Fig. 4, where

$\epsilon \in \{0, 0.1, 0.2, 0.4\}$ and $\epsilon = 0$ means accurate class priors. It can be obviously observed that the proposed method is rarely affected by the noisy class priors and can be safely applied in the wild.

5 Conclusions

In this work, we focused on learning from multiple unlabeled datasets and proposed a new method based on a surrogate set classification task. We first bridged the surrogate and original class-posterior probabilities via a linear-fractional transformation, and then studied its properties. Based on them, we proposed the U^m -SSC algorithm and implemented it by adding an adaptation layer to the neural network. We theoretically proved that the proposed method is classifier-consistent and established an estimation error bound for it. Experiments also demonstrated that the proposed method outperforms state-of-the-art methods and is robust in more challenging experimental setups.

Acknowledgments

We thank Wenkai Xu, Tianyi Zhang, Nontawat Charoenphakdee and Yuting Tang for helpful discussion. NL was supported by MEXT scholarship No. 171536 and the MSRA D-CORE Program. GN and MS were supported by JST AIP Acceleration Research Grant Number JPMJCR20U3, Japan. MS was also supported by Institute for AI and Beyond, UTokyo.

References

D. M. Allen. Mean square error of prediction as a criterion for selecting variables. *Technometrics*, 13(3):469–475, 1971.

H. Bao, G. Niu, and M. Sugiyama. Classification from pairwise similarity and unlabeled data. In *ICML*, 2018.

P. L. Bartlett, M. I. Jordan, and J. D. McAuliffe. Convexity, classification, and risk bounds. *Journal of the American Statistical Association*, 101(473):138–156, 2006.

S. Ben-David, N. Eiron, and P. Long. On the difficulty of approximately maximizing agreements. *Journal of Computer and System Sciences*, 66(3):496–514, 2003.

D. P. Bertsekas. Nonlinear programming. *Journal of the Operational Research Society*, 48(3):334–334, 1997.

K. H. Brodersen, C. S. Ong, K. E. Stephan, and J. M. Buhmann. The balanced accuracy and its posterior distribution. In *ICPR*, 2010.

T. Clanuwat, M. Bober-Irizar, A. Kitamoto, A. Lamb, K. Yamamoto, and D. Ha. Deep learning for classical Japanese literature. *arXiv preprint arXiv:1812.01718*, 2018.

P.-T. De Boer, D. P. Kroese, S. Mannor, and R. Y. Rubinstein. A tutorial on the cross-entropy method. *Annals of operations research*, 134(1):19–67, 2005.

J. Edmonds. Maximum matching and a polyhedron with 0, 1-vertices. *Journal of research of the National Bureau of Standards B*, 69(125-130):55–56, 1965.

J. Edmonds and R. M. Karp. Theoretical improvements in algorithmic efficiency for network flow problems. *Journal of the ACM (JACM)*, 19(2):248–264, 1972.

L. Feng, T. Kaneko, B. Han, G. Niu, B. An, and M. Sugiyama. Learning with multiple complementary labels. In *ICML*, 2020.

I. Goodfellow, Y. Bengio, and A. Courville. *Deep Learning*. MIT Press, 2016.

K. He, X. Zhang, S. Ren, and J. Sun. Deep residual learning for image recognition. In *CVPR*, 2016.

S. Ioffe and C. Szegedy. Batch normalization: Accelerating deep network training by reducing internal covariate shift. *arXiv preprint arXiv:1502.03167*, 2015.

T. Ishida, G. Niu, W. Hu, and M. Sugiyama. Learning from complementary labels. In *NeurIPS*, 2017.

T. Ishida, G. Niu, A. K. Menon, and M. Sugiyama. Complementary-label learning for arbitrary losses and models. In *ICML*, 2019.

D. P. Kingma and J. Ba. Adam: A method for stochastic optimization. *arXiv preprint arXiv:1412.6980*, 2014.

D. P. Kingma and J. L. Ba. Adam: A method for stochastic optimization. In *ICLR*, 2015.

A. Krizhevsky. Learning multiple layers of features from tiny images. Technical report, University of Toronto, 2009.

Y. LeCun, L. Bottou, Y. Bengio, and P. Haffner. Gradient-based learning applied to document recognition. *Proceedings of the IEEE*, 86(11):2278–2324, 1998.

M. Li and Z. Zhou. Improve computer-aided diagnosis with machine learning techniques using undiagnosed samples. *IEEE Transactions on Systems, Man, and Cybernetics-Part A: Systems and Humans*, 37(6):1088–1098, 2007.

T. Liu and D. Tao. Classification with noisy labels by importance reweighting. *IEEE Transactions on Pattern Analysis and Machine Intelligence*, 38(3):447–461, 2016.

N. Lu, G. Niu, A. K. Menon, and M. Sugiyama. On the minimal supervision for training any binary classifier from only unlabeled data. In *ICLR*, 2019.

N. Lu, T. Zhang, G. Niu, and M. Sugiyama. Mitigating overfitting in supervised classification from two unlabeled datasets: A consistent risk correction approach. In *AISTATS*, 2020.

A. Maurer. A vector-contraction inequality for rademacher complexities. In *ALT*, pages 3–17. Springer, 2016.

C. McDiarmid. On the method of bounded differences. *Surveys in combinatorics*, 141(1):148–188, 1989.

A. K. Menon, B. van Rooyen, C. S. Ong, and R. C. Williamson. Learning from corrupted binary labels via class-probability estimation. In *ICML*, 2015.

N. Natarajan, I. S. Dhillon, P. Ravikumar, and A. Tewari. Learning with noisy labels. In *NeurIPS*, 2013.

G. Patrini, R. Nock, P. Rivera, and T. Caetano. (almost) no label no cry. *NeurIPS*, 2014.

G. Patrini, A. Rozza, A. K. Menon, R. Nock, and L. Qu. Making deep neural networks robust to label noise: A loss correction approach. In *CVPR*, 2017.

N. Quadrianto, A. J. Smola, T. S. Caetano, and Q. V. Le. Estimating labels from label proportions. *Journal of Machine Learning Research*, 10:2349–2374, 2009.

C. Scott and J. Zhang. Learning from label proportions: A mutual contamination framework. In *NeurIPS*, 2020.

S. Shalev-Shwartz and S. Ben-David. *Understanding Machine Learning: From Theory to Algorithms*. Cambridge University Press, 2014.

N. Srivastava, G. Hinton, A. Krizhevsky, I. Sutskever, and R. Salakhutdinov. Dropout: a simple way to prevent neural networks from overfitting. *Journal of machine learning research*, 15(1):1929–1958, 2014.

K.-H. Tsai and H.-T. Lin. Learning from label proportions with consistency regularization. In *ACML*, 2020.

V. N. Vapnik. *Statistical Learning Theory*. John Wiley & Sons, 1998.

H. Xiao, K. Rasul, and R. Vollgraf. Fashion-MNIST: a novel image dataset for benchmarking machine learning algorithms. *arXiv preprint arXiv:1708.07747*, 2017.

L. Xu, J. Honda, G. Niu, and M. Sugiyama. Uncoupled regression from pairwise comparison data. In *NeurIPS*, 2019.

F. X. Yu, D. Liu, S. Kumar, T. Jebara, and S.-F. Chang. \propto SVM for learning with label proportions. In *ICML*, 2013.

F. X. Yu, K. Choromanski, S. Kumar, T. Jebara, and S.-F. Chang. On learning from label proportions. *arXiv preprint arXiv:1402.5902*, 2014.

Supplementary Material

A Proofs

In this appendix, we prove all theorems.

A.1 Proof of Theorem 1

On one hand, $\forall j \in [1, \dots, m]$ we have:

$$\begin{aligned}\bar{\eta}_j(\mathbf{x}) &= \frac{p(\mathbf{x}, \bar{y} = j)}{\bar{p}(\mathbf{x})} \\ &= \frac{p(\mathbf{x} \mid \bar{y} = j) \cdot p(\bar{y})}{\bar{p}(\mathbf{x})} = j \\ &= \frac{\rho_j \cdot [\pi_j \cdot p_p(\mathbf{x}) + (1 - \pi_j) \cdot p_n(\mathbf{x})]}{\sum_{j=1}^m \rho_j \cdot [\pi_j \cdot p_p(\mathbf{x}) + (1 - \pi_j) \cdot p_n(\mathbf{x})]}. \end{aligned} \quad (18)$$

The third equality is due to the definition of $p(\mathbf{x} \mid \bar{y} = j)$ and we substitute it with p_{tr} that is defined in Eq. (3). On the other hand, by Bayes' rule we have:

$$\begin{aligned}p_p(\mathbf{x}) &= p(\mathbf{x} \mid y = +1) = \frac{p(y = +1 \mid \mathbf{x}) \cdot p(\mathbf{x})}{p(y = +1)} = \frac{\eta(\mathbf{x}) \cdot p(\mathbf{x})}{\pi_{\mathcal{D}}}, \\ p_n(\mathbf{x}) &= p(\mathbf{x} \mid y = -1) = \frac{p(y = -1 \mid \mathbf{x}) \cdot p(\mathbf{x})}{p(y = -1)} = \frac{(1 - \eta(\mathbf{x})) \cdot p(\mathbf{x})}{1 - \pi_{\mathcal{D}}}. \end{aligned} \quad (19)$$

Plug Eq. (19) into Eq. (18) and multiply $\pi_{\mathcal{D}} \cdot (1 - \pi_{\mathcal{D}})$ on both numerator and denominator we obtain:

$$\begin{aligned}\bar{\eta}_j(\mathbf{x}) &= \frac{\rho_j \cdot [\pi_j \eta(\mathbf{x}) \cdot (1 - \pi_{\mathcal{D}}) + (1 - \pi_j) \cdot (1 - \eta(\mathbf{x})) \cdot \pi_{\mathcal{D}}]}{\sum_{j=1}^m \rho_j \cdot [\pi_j \eta(\mathbf{x}) \cdot (1 - \pi_{\mathcal{D}}) + (1 - \pi_j) \cdot (1 - \eta(\mathbf{x})) \cdot \pi_{\mathcal{D}}]} \\ &= \frac{\rho_j \cdot (\pi_j - \pi_{\mathcal{D}}) \cdot \eta(\mathbf{x}) + \rho_j \cdot (1 - \pi_j) \cdot \pi_{\mathcal{D}}}{\sum_{j=1}^m \rho_j \cdot (\pi_j - \pi_{\mathcal{D}}) \cdot \eta(\mathbf{x}) + \sum_{j=1}^m \rho_j \cdot (1 - \pi_j) \cdot \pi_{\mathcal{D}}}. \end{aligned}$$

By setting the coefficients a_j, b_j, c, d accordingly we conclude the proof. \square

A.2 Proof of Lemma 2

We proceed the proof by first showing that the denominators in each function $Q_j(t)$ for $j = 1, \dots, m$ is strictly greater than zero for all $t \in [0, 1]$. And then show that $\mathbf{Q}(t_1) = \mathbf{Q}(t_2)$ if and only if $t_1 = t_2$.

For all $j = 1, \dots, m$, the denominator of $Q_j(t)$ is same and equal to $c \cdot t + d$ where $c = \sum_{j=1}^m \rho_j(\pi_j - \pi_{\mathcal{D}})$ and $d = \sum_{j=1}^m \rho_j \pi_{\mathcal{D}}(1 - \pi_j)$. d is positive since $\rho_j > 0, \pi_{\mathcal{D}} > 0$ and there exists $j \in 1, \dots, m$ such that $\pi_j < 1$. Given that $t \in [0, 1]$, we discuss the sign of c as follows:

1. when $c \geq 0$, the minimum value of $c \cdot t + d$ is $c \cdot 0 + d = d > 0$;
2. when $c < 0$, the minimum value of $c \cdot t + d$ is $c \cdot 1 + d = \sum_{j=1}^m \rho_j(\pi_j - \pi_{\mathcal{D}}) + \sum_{j=1}^m \rho_j \pi_{\mathcal{D}}(1 - \pi_j) = \sum_{j=1}^m \rho_j \pi_j(1 - \pi_{\mathcal{D}}) > 0$, where the last inequality is due to the existence of $j \in 1, \dots, m$ such that $\pi_j > 0$.

Hitherto, the denominator $c \cdot t + d > 0$ is shown. Next, we prove the one-to-one mapping property. Assume that there are $t_1, t_2 \in [0, 1]$ such that $\mathbf{Q}(t_1) = \mathbf{Q}(t_2)$, it indicates that $Q_j(t_1) = Q_j(t_2), \forall j = 1, \dots, m$. For all j , we get

$$\begin{aligned} Q_j(t_1) - Q_j(t_2) &= \frac{a_j \cdot t_1 + b_j}{c \cdot t_1 + d} - \frac{a_j \cdot t_2 + b_j}{c \cdot t_2 + d} \\ &= \frac{(a_j \cdot t_1 + b_j)((c \cdot t_2 + d)) - (a_j \cdot t_2 + b_j)((c \cdot t_1 + d))}{(c \cdot t_1 + d)(c \cdot t_2 + d)} \\ &= \frac{(t_1 - t_2)(a_j \cdot d - b_j \cdot c)}{(c \cdot t_1 + d)(c \cdot t_2 + d)} = 0, \end{aligned} \quad (20)$$

where $a_j = \rho_j \cdot (\pi_j - \pi_{\mathcal{D}})$ and $b_j = \rho_j \cdot (1 - \pi_j) \cdot \pi_{\mathcal{D}}$. As shown before, the denominator of equation 20 is not zero, we next show that there is at least one $i \in 1, \dots, m, a_j \cdot d - b_j \cdot c \neq 0$. Since c and d are constants and irrelevant to i , we get

$$\begin{aligned} a_j \cdot d - b_j \cdot c &= (\rho_j \cdot (\pi_j - \pi_{\mathcal{D}})) \cdot d - (\rho_j \cdot (1 - \pi_j) \cdot \pi_{\mathcal{D}}) \cdot c \\ &= \rho_j \cdot (\pi_j \cdot d - \pi_{\mathcal{D}} \cdot d - c + \pi_j \cdot c) \\ &= \pi_j \cdot (c + d) - \pi_{\mathcal{D}} \cdot d - c. \end{aligned}$$

This equation equals to zero if and only if $\pi_j = \frac{c + \pi_{\mathcal{D}} \cdot d}{c + d}$, but according to our assumption that at least two of the U sets are different, $\exists j' \in 1, \dots, m$ such that $\pi_{j'} \neq \frac{c + \pi_{\mathcal{D}} \cdot d}{c + d}$. For such j' , $Q_{j'}(t_1) = Q_{j'}(t_2)$ if and only if $t_1 = t_2$. We conclude the proof. \square

A.3 Proof of Lemma 3

We provide proof of cross-entropy and mean square loss functions, which are very commonly used losses for classification problems because of their numerical stability and good convergence rate De Boer et al. (2005); Allen (1971).

cross-entropy Loss Since cross-entropy loss is non-negative according to it's definition, minimizing $R_{\text{Surr}}(\mathbf{g})$ can be obtained by minimizing the conditional risk $\mathbb{E}_{p(\bar{y}|\mathbf{x})}[\ell(\mathbf{g}(\mathbf{x}), \bar{y}) \mid \mathbf{x}]$ for every $\mathbf{x} \in \mathcal{X}$. In a word, we are now optimizing

$$\phi(\mathbf{g}) = - \sum_{j=1}^m p(\bar{y} = j \mid \mathbf{x}) \cdot \log(g_j(\mathbf{x})), \quad \text{s.t. } \sum_{j=1}^m g_j(\mathbf{x}) = 1.$$

By using Lagrange Multiplier method Bertsekas (1997), we have:

$$\mathcal{L} = - \sum_{j=1}^m p(\bar{y} = j \mid \mathbf{x}) \cdot \log(g_j(\mathbf{x})) - \lambda \cdot \left(\sum_{j=1}^m g_j(\mathbf{x}) - 1 \right).$$

The derivative of \mathcal{L} with respect to \mathbf{g} is:

$$\frac{\partial \mathcal{L}}{\partial \mathbf{g}} = \left[-\frac{p(\bar{y} = 1 \mid \mathbf{x})}{g_1(\mathbf{x})} - \lambda, \dots, -\frac{p(\bar{y} = m \mid \mathbf{x})}{g_m(\mathbf{x})} - \lambda \right]^\top.$$

By setting this derivative to 0 we obtain:

$$g_j(\mathbf{x}) = -\lambda p(\bar{y} = j \mid \mathbf{x}), \quad \forall j = 1, \dots, m \text{ and } \forall \mathbf{x} \in \mathcal{X}.$$

Since $\mathbf{g} \in \Delta^{m-1}$ is the m -dimensional simplex, we have $\sum_{j=1}^m g_j^*(\mathbf{x}) = 1$ and $\sum_{j=1}^m p(\bar{y} = j \mid \mathbf{x}) = 1$, then,

$$\sum_{j=1}^m g_j^*(\mathbf{x}) = -\lambda \cdot \sum_{j=1}^m p(\bar{y} = j \mid \mathbf{x}) = 1.$$

Therefore we obtain $\lambda = -1$ and $g_j^*(\mathbf{x}) = p(\bar{y} = j \mid \mathbf{x}) = \bar{\eta}_j(\mathbf{x})$, $\forall j = 1, \dots, m$ and $\forall \mathbf{x} \in \mathcal{X}$, which is equivalent to $\mathbf{g}^* = \bar{\boldsymbol{\eta}}$. Note that when $m = 2$, the softmax is reduce to sigmoid function and the cross-entropy is reduced to logistic loss $\ell_{\log}(z) = \ln(1 + \exp(-z))$.

Mean Square Error Similar to cross-entropy loss, we transform the minimization problem to the following constrained optimization problem:

$$\phi(\mathbf{g}) = \sum_{j=1}^m (p(\bar{y} = j \mid \mathbf{x}) - g_j(\mathbf{x}))^2, \quad \text{s.t. } \sum_{j=1}^m g_j(\mathbf{x}) = 1.$$

By using the Lagrange multiplier method, we obtain:

$$\mathcal{L} = \sum_{j=1}^m (p(\bar{y} = j \mid \mathbf{x}) - g_j(\mathbf{x}))^2 - \lambda \cdot \left(\sum_{j=1}^m g_j(\mathbf{x}) - 1 \right).$$

By setting the derivative of \mathcal{L} with respect to \mathbf{g} to 0, we get:

$$g_j(\mathbf{x}) = p(\bar{y} = j \mid \mathbf{x}) + \frac{\lambda}{2}.$$

Since $\sum_{j=1}^m g_j^*(\mathbf{x}) = 1$ and $\sum_{j=1}^m p(\bar{y} = j \mid \mathbf{x}) = 1$, we have:

$$\begin{aligned} \sum_{j=1}^m g_j^*(\mathbf{x}) &= \sum_{j=1}^m p(\bar{y} = j \mid \mathbf{x}) - \frac{\lambda \cdot m}{2}, \\ &= -\frac{\lambda \cdot m}{2} = 0. \end{aligned}$$

Since $m \geq 2$, we can obtain $\lambda = 0$. Consequently, $g_j^*(\mathbf{x}) = p(\bar{y} = j \mid \mathbf{x}) = \bar{\eta}_j(\mathbf{x})$, which leads to $\mathbf{g}^* = \bar{\boldsymbol{\eta}}$ and concludes the proof. \square

A.4 Proof of Theorem 4

Proof. According to Lemma 3, when cross-entropy or mean square error is used as the loss function ℓ , the mapping $\mathbf{g}^*(\mathbf{x}) = \bar{\eta}(\mathbf{x})$ uniquely minimizes $R_{\text{Surr}}(\mathbf{g}; \ell)$. Thus by denoting $\mathbf{q}(\mathbf{x}) = \mathbf{Q}(f(\mathbf{x}))$, $R_{\text{Surr}}(\mathbf{q}(\mathbf{x})) = \mathbb{E}_{(\mathbf{x}, \bar{y}) \sim \bar{\mathcal{D}}}[\ell(\mathbf{q}(\mathbf{x}), \bar{y})]$ is minimized if and only if $\mathbf{q}(\mathbf{x}) = \bar{\eta}(\mathbf{x}) = \mathbf{g}^*(\mathbf{x})$. Combining Theorem 1 and Lemma 2 we get $\mathbf{q}(\mathbf{x}) = \bar{\eta}(\mathbf{x})$ if and only if $f(\mathbf{x}) = \eta(\mathbf{x})$. As the result, induced by $\mathbf{g}^* = \operatorname{argmin}_{\mathbf{g}} R_{\text{Surr}}(\mathbf{g})$, we have $\eta(\mathbf{x}) = \operatorname{argmin}_f R_{\text{Surr}}(f) = f_{\text{Surr}}^*(\mathbf{x})$.

On the other hand, when ℓ_b is a softmax cross-entropy (logistic loss for binary case) or mean squared loss, the mapping f_{Surr}^* is a unique minimizer of $R(f; \ell_b)$. We skip the proof since it is similar to the proof of Lemma 3. Then, we get $f_{\text{Surr}}^*(\mathbf{x}) = \eta(\mathbf{x}) = f^*(\mathbf{x})$, which concludes the proof. \square

A.5 Proof of Lemma 5

For any $j \in 1, \dots, m$, by taking derivative of $Q_j(f)$ with respect to f , we get

$$\left| \frac{\partial Q_j}{\partial f} \right| = \left| \frac{a_j d - b_j c}{(c \cdot f + d)^2} \right| = \frac{|a_j d - b_j c|}{(c \cdot f + d)^2}, \quad (17)$$

where all the coefficients are as denoted in Theorem 1,

$$a_j = \rho_j(\pi_j - \pi_{\mathcal{D}}), \quad b_j = \rho_j \pi_{\mathcal{D}}(1 - \pi_j), \quad c = \sum_{j=1}^m \rho_j(\pi_j - \pi_{\mathcal{D}}), \quad d = \sum_{j=1}^m \rho_j \pi_{\mathcal{D}}(1 - \pi_j).$$

Since for all class priors we have $0 \leq \pi_j \leq 1$, $0 < \pi_{\mathcal{D}} < 1$, $0 < \rho_j < 1$ and $\sum_{j=1}^m (\rho_j) = 1$. It's obvious that

$$-1 \leq a_j \leq 1, \quad 0 \leq b_j \leq 1, \quad 1 \leq c \leq 1 \text{ and } 0 \leq d \leq 1.$$

Therefore, for the nominator of the Equation (A.5) we have

$$|a_j d - b_j c| \leq 2. \quad (15)$$

On the other hand, since $d > 0$ and $0 \leq f \leq 1$, by substituting $f = 0$ and $f = 1$ respectively, we can get

$$\begin{aligned} c \cdot f + d &\geq c + d = \sum_{j=1}^m \rho_j \pi_j (1 - \pi_{\mathcal{D}}) > 0, \text{ if } c < 0 \\ c \cdot f + d &\geq d > 0, \text{ if } c \geq 0 \end{aligned}$$

In general, we lower bound the term by $c \cdot f + d \geq \min(c + d, d) > 0$. As the result, we can bound the denominator of Equation (A.5)

$$\begin{aligned} (c \cdot f + d)^2 &\geq (\min(c + d, d))^2 \\ &= \left(\min \left(\sum_{j=1}^m \rho_j \pi_j (1 - \pi_{\mathcal{D}}), \sum_{j=1}^m \rho_j \pi_{\mathcal{D}} (1 - \pi_j) \right) \right)^2 \\ &= \alpha^2. \end{aligned}$$

Then, by combining Equation (A.5) and Equation (A.5), we have

$$\left| \frac{\partial Q_j}{\partial f} \right| \leq \frac{2}{\alpha^2}$$

This bound illustrates that $Q_j(f(\mathbf{x}))$ is $2/\alpha^2$ -Lipschitz-continuous with respect to $f(\mathbf{x})$ and we complete the proof. \square

A.6 Proof of Theorem 6

We first introduce the following conclusion connecting the estimation error bound and the generalization error bound.

Lemma 7. *Denote by \mathcal{F} the hypothesis class, the estimation error $R_{\text{Surr}}(\hat{f}_{\text{Surr}}) - R_{\text{Surr}}(f_{\text{Surr}}^*)$ is bounded by*

$$R_{\text{Surr}}(\hat{f}_{\text{Surr}}) - R_{\text{Surr}}(f_{\text{Surr}}^*) \leq 2 \sup_{f \in \mathcal{F}} |R_{\text{Surr}}(f) - \hat{R}_{\text{Surr}}(f)|.$$

Proof. We use the commonly used proof procedure of constructing inequalities:

$$\begin{aligned} R_{\text{Surr}}(\hat{f}_{\text{Surr}}) - R_{\text{Surr}}(f_{\text{Surr}}^*) &= (R_{\text{Surr}}(\hat{f}_{\text{Surr}}) - \hat{R}_{\text{Surr}}(\hat{f}_{\text{Surr}})) \\ &\quad + (\hat{R}_{\text{Surr}}(\hat{f}_{\text{Surr}}) - \hat{R}_{\text{Surr}}(f_{\text{Surr}}^*)) \\ &\quad + (\hat{R}_{\text{Surr}}(f_{\text{Surr}}^*) - R_{\text{Surr}}(f_{\text{Surr}}^*)) \\ &\leq R_{\text{Surr}}(\hat{f}_{\text{Surr}}) - \hat{R}_{\text{Surr}}(\hat{f}_{\text{Surr}}) + \hat{R}_{\text{Surr}}(f_{\text{Surr}}^*) - R_{\text{Surr}}(f_{\text{Surr}}^*) \\ &\leq 2 \sup_{f \in \mathcal{F}} |R_{\text{Surr}}(f) - \hat{R}_{\text{Surr}}(f)|. \end{aligned}$$

We complete the proof. \square

Lemma 7 uses the generalization error to bound the estimation error of the ERM algorithm. Then, we consider the generalization error bound.

Lemma 8. *Let $\mathbf{g} \in \mathcal{G}$, where $\mathcal{G} = \{\mathbf{x} \mapsto \mathbf{Q}(f(\mathbf{x})) \mid f \in \mathcal{F}\}$ is a class of measurable functions. Let $\mathfrak{R}_{n_{\text{tr}}}(\ell \circ \mathcal{G})$ be the Rademacher complexity on $\ell \circ \mathcal{G}$ when n_{tr} samples are given, i.e.,*

$$\mathfrak{R}_{n_{\text{tr}}}(\ell \circ \mathcal{G}) = \mathbb{E} \left[\sup_{f \in \mathcal{G}} \frac{1}{n_{\text{tr}}} \sum_{i=1}^{n_{\text{tr}}} \sigma_i \ell(\mathbf{g}(\mathbf{x}_i), \bar{y}_i) \right],$$

where $\{\sigma_1, \dots, \sigma_{n_{\text{tr}}}\}$ are Rademacher variables uniformly distributed from $\{-1, 1\}$. And we assume $\ell(\mathbf{g}(\mathbf{x}), \bar{y})$ is upper-bounded by M_ℓ . Then, for any $\delta > 0$, with probability at least $1 - \delta$ we have

$$\sup_{\mathbf{g} \in \mathcal{G}} |R_{\text{Surr}}(\mathbf{g}) - \hat{R}_{\text{Surr}}(\mathbf{g})| \leq 2\mathfrak{R}_{n_{\text{tr}}}(\ell \circ \mathcal{G}) + M_\ell \sqrt{\frac{\log(1/\delta)}{2n_{\text{tr}}}}.$$

Proof. We consider the one-side uniform deviation $\sup_{\mathbf{g} \in \mathcal{G}} R_{\text{Surr}}(\mathbf{g}) - \hat{R}_{\text{Surr}}(\mathbf{g})$. Let (\mathbf{x}, \bar{y}) be randomly sampled from $\bar{\mathcal{D}}$. Then, suppose an sample $(\mathbf{x}_i, \bar{y}_i)$ is replaced by another arbitrary sample $(\mathbf{x}_j, \bar{y}_j)$, the change of $\sup_{\mathbf{g} \in \mathcal{G}} R_{\text{Surr}}(\mathbf{g}) - \hat{R}_{\text{Surr}}(\mathbf{g})$ is no greater than M_ℓ/n_{tr} since the loss $\ell(\cdot)$ is bounded by M_ℓ . By applying McDiarmid's inequality [McDiarmid \(1989\)](#), for any $\delta > 0$, with probability at least $1 - \delta/2$,

$$\sup_{\mathbf{g} \in \mathcal{G}} R_{\text{Surr}}(\mathbf{g}) - \hat{R}_{\text{Surr}}(\mathbf{g}) \leq \mathbb{E} \left[\sup_{\mathbf{g} \in \mathcal{G}} R_{\text{Surr}}(\mathbf{g}) - \hat{R}_{\text{Surr}}(\mathbf{g}) \right] + M_\ell \sqrt{\frac{\log(1/\delta)}{2n_{\text{tr}}}}.$$

It is a routine work to derive that

$$\mathbb{E} \left[\sup_{\mathbf{g} \in \mathcal{G}} R_{\text{Surr}}(\mathbf{g}) - \hat{R}_{\text{Surr}}(\mathbf{g}) \right] \leq 2\mathfrak{R}_{n_{\text{tr}}}(\ell \circ \mathcal{G}).$$

The bound for the other side can be similarly shown due to symmetrization [Vapnik \(1998\)](#). By combining the two sides' inequalities, we complete the proof. \square

Then, we upper-bound $\mathfrak{R}_{n_{\text{tr}}}(\ell \circ \mathcal{G})$. Since $\ell(\mathbf{g}(\mathbf{x}), \bar{y})$ is \mathcal{L}_ℓ -Lipschitz continuous w.r.t \mathbf{g} . According to Talagrand's contraction lemma [Shalev-Shwartz and Ben-David \(2014\)](#) and the Rademacher vector contraction inequality [Maurer \(2016\)](#), we have

$$\begin{aligned} \mathfrak{R}_{n_{\text{tr}}}(\ell \circ \mathcal{G}) &\leq \sqrt{2}\mathcal{L}_\ell \cdot \mathbb{E} \left[\sup_{\mathbf{g} \in \mathcal{G}} \sum_{j=1}^m \sum_{i=1}^{n_j} \epsilon_{ij} g_j(\mathbf{x}_i) \right] \\ &\leq \sum_{j=1}^m \mathbb{E} \left[\sup_{\mathbf{g} \in \mathcal{G}} \sum_{i=1}^{n_j} \epsilon_i g_j(\mathbf{x}_i) \right], \end{aligned}$$

where $g_j(\mathbf{x}_i)$ is the j -th component of $\mathbf{g}(\mathbf{x}_i)$. Since $g_j(\mathbf{x}) = Q_j(f(\mathbf{x}))$ and $Q_j(f)$ is Lipschitz continuous w.r.t f with a Lipschitz constant $2/\alpha^2$, applying again the Talagrand's contraction lemma [Shalev-Shwartz and Ben-David \(2014\)](#), we have

$$\begin{aligned} \sum_{j=1}^m \mathbb{E} \left[\sup_{\mathbf{g} \in \mathcal{G}} \sum_{i=1}^{n_j} \epsilon_i g_j(\mathbf{x}_i) \right] &= \sum_{j=1}^m \mathbb{E} \left[\sup_{f \in \mathcal{F}} \sum_{i=1}^{n_j} \epsilon_i Q_j(f(\mathbf{x}_i)) \right] \\ &\leq \frac{2}{\alpha^2} \sum_{j=1}^m \mathbb{E} \left[\sup_{f \in \mathcal{F}} \sum_{i=1}^{n_j} \epsilon_i f(\mathbf{x}_i) \right] \\ &= \frac{2}{\alpha^2} \sum_{j=1}^m \mathfrak{R}_{n_j}(\mathcal{F}). \end{aligned}$$

Combining with Eq. (A.6), Lemma 7, and Lemma 8, we get that with probability at least $1 - \delta$, the

estimation error bound

$$\begin{aligned}
R_{\text{Surr}}(\hat{f}_{\text{Surr}}) - R_{\text{Surr}}(f_{\text{Surr}}^*) &\leq 2 \sup_{f \in \mathcal{F}} |R_{\text{Surr}}(f) - \hat{R}_{\text{Surr}}(f)| \\
&= 2 \sup_{\mathbf{g} \in \mathcal{G}} |R_{\text{Surr}}(\mathbf{g}) - \hat{R}_{\text{Surr}}(\mathbf{g})| \\
&\leq 4 \mathfrak{R}_{n_{\text{tr}}}(\ell \circ \mathcal{G}) + M_\ell \sqrt{\frac{\log(1/\delta)}{2n_{\text{tr}}}} \\
&\leq \frac{4\sqrt{2}\mathcal{L}_\ell}{\alpha^2} \sum_{j=1}^m \mathfrak{R}_{n_j}(\mathcal{F}) + M_\ell \sqrt{\frac{\log(1/\delta)}{2n_{\text{tr}}}}
\end{aligned}$$

Note that $\sup_{\mathbf{g} \in \mathcal{G}} |R_{\text{Surr}}(\mathbf{g}) - \hat{R}_{\text{Surr}}(\mathbf{g})| = \sup_{f \in \mathcal{F}} |R_{\text{Surr}}(f) - \hat{R}_{\text{Surr}}(f)|$ is because $\mathcal{G} = \{\mathbf{x} \mapsto \mathbf{Q}(f(\mathbf{x})) \mid f \in \mathcal{F}\}$ and $\mathbf{Q}(\cdot)$ is deterministic. Since Theorem 4 shows that $f_{\text{Surr}}^* = f^*$, we can substitute f_{Surr}^* by f^* and get

$$R_{\text{Surr}}(\hat{f}_{\text{Surr}}) - R_{\text{Surr}}(f^*) \leq \frac{4\sqrt{2}\mathcal{L}_\ell}{\alpha^2} \sum_{j=1}^m \mathfrak{R}_{n_j}(\mathcal{F}) + M_\ell \sqrt{\frac{\log(1/\delta)}{2n_{\text{tr}}}}.$$

The proof is completed. \square

B Supplementary Information on the Experiments

B.1 Datasets

The following are the details of the datasets and dividing process.

MNIST This is a dataset of normalized grayscale images containing handwritten digits from 0 to 9. All the images are fitted into a 28×28 pixels. The total number of training images and test images is 60,000 and 10,000 respectively. We use the even digits as the positive class and odd digits as the negative class.

Fashion-MNIST This is a dataset of grayscale images of different types of modern clothes. All the images are of the size 28×28 pixels. Similar to MNIST, this dataset has 60,000 training images and 10,000 test images. We convert all this 10-classes dataset into a binary dataset as follows:

- The classes ‘Pullover’, ‘Dress’, ‘T-shirt’, ‘Trouser’, ‘Shirt’, ‘Bag’, ‘Ankle boot’ and ‘Sneaker’ are denoted as the positive class.
- The classes ‘Coat’ and ‘Sandal’ are denoted as the negative class.

Kuzushiji-MNIST This is a dataset of grayscale images of cursive Japanese (Kuzushiji) characters. This dataset also has all images of size 28×28 . And the total number of training images and test images is 60,000 and 10,000 respectively. For Kuzushiji-MNIST dataset, we convert it to the binary dataset as:

- The classes ‘ki’, ‘re’, and ‘wo’ are denoted as the positive class.
- The classes ‘o’, ‘su’, ‘tsu’, ‘na’, ‘ha’, ‘ma’, and ‘ya’ are denoted as the negative class.

CIFAR-10 This dataset is made up of color images of different types of objects and animals. The size of all images in this dataset is 32×32 . There are 5,000 training images and 1,000 test images For every class so in total 50,000 training and 10,000 test images. For this dataset, we use the following dividing process:

- The positive class consists of ‘airplane’, ‘bird’, ‘deer’, ‘dog’, ‘frog’, ‘cat’, and ‘horse’.
- The negative class consists of ‘automobile’, ‘ship’, and ‘truck’.

The generation methods of the U sets are the same for all four datasets. In particular, given the number of U sets m , and class prior π_i and set size n_i for the U set i , we go through the following process:

1. shuffle the dataset;
2. randomly pick (with replacement) $n_i^p = n_i \times \pi_i$ samples of positive class;
3. randomly pick (with replacement) $n_i^n = n_i - n_i^p$ samples of negative class;
4. combine them with chosen positive samples to form set i .

B.2 Models

We used two models of deep neural networks for the experiments. Here we introduce the structure of the models and specify the hyper-parameters.

MLP The first model is a 5-layer fully connected perceptron with ReLU as the activation function. The model is $d - 300 - 300 - 300 - 1$, where d is the dimension of the input feature. Batch normalization [Ioffe and Szegedy \(2015\)](#) was applied for each hidden layer and ℓ_2 -regularization was added. A dropout [Srivastava et al. \(2014\)](#) layer of rate 0.2 is added before every hidden layer. The optimizer was Adam [Kingma and Ba \(2014\)](#) with the default momentum parameters ($\beta_1 = 0.9$ and $\beta_2 = 0.999$).

ResNet-32 The second model is a 32-layer residual networks [He et al. \(2016\)](#) as follows:

0th (input) layer: $(32 * 32 * 3) -$

1st to 11th layers: $C(3 * 3, 16) - [C(3 * 3, 16), C(3 * 3, 16)] * 5 -$

12th to 21st layers: $[C(3 * 3, 32), C(3 * 3, 32)] * 5 -$

22nd to 31st layers: $[C(3 * 3, 64), C(3 * 3, 64)] * 5 -$

32nd layer: Global Average Pooling-1,

where $C(3 * 3, 96)$ represents a 96-channel of $3 * 3$ convolutions followed by an activation function ReLU, $[\cdot] * 2$ represents a repeat of twice of such layer. $C(3 * 3, 96, 2)$ represents a similar layer but with stride 2, $[\cdot, \cdot]$ represents a building block. Batch normalization was applied for each hidden

layers and ℓ_2 -regularization was also added. The optimizer was Adam with the default momentum parameters ($\beta_1 = 0.9$ and $\beta_2 = 0.999$).

We applied the MLP model for MNIST, Fashion-MNIST, Kuzushiji-MNIST, and applied the ResNet-32 model for the CIFAR-10 dataset.

B.3 Other Details

Training details We implemented all methods by Keras and conducted all the experiments on an NVIDIA Tesla P100 GPU. For all 4 datasets, the learning rate decay is $1e-4$ for all 4 methods. The batch size is 256 for U^m -SSC, MMC-unbiased and MMC-ReLU methods. For the MNIST, the Fashion-MNIST, and the Kuzushiji MNIST dataset, the learning-rate is $1e-5$ for U^m -SSC, $1e-4$ for MMC-unbiased, MMC-ReLU, and LLP-VAT. for the CIFAR-10 dataset, the learning-rate is $5e-6$ for U^m -SSC, $1e-5$ for MMC-unbiased, MMC-ReLU, and LLP-VAT methods. Note that we set the hyper-parameters $\alpha = 0.05$ and $\epsilon = 6.0$ for LLP-VAT following the default implementation of their paper [Tsai and Lin \(2020\)](#).

Comparison with State-of-the-art Methods Setup In this experiment, the set sizes are uniform. To be clear, since, for each dataset, the total number of training samples T is fixed ($T=60,000$ in MNIST, Fashion-MNIST, and Kuzushiji-MNIST, $T=50,000$ in CIFAR-10), the number of instances contained in each set is also fixed as T/m .

Since the set sizes are the same across all sets. The paring of U sets for MMC-unbiased and MMC-ReLU methods are according to Proposition 15 in [Scott and Zhang \(2020\)](#), i.e., matching the set with largest π_i with the smallest, the second-largest π_i with the second smallest, and so on.

C Supplementary Experimental Results

C.1 Comparison with State-of-the-art Methods Results

Table 4 reports the test performance of each method using the same model on corresponding benchmark datasets.

C.2 On the training loss Results

We find the training loss of the proposed U^m -SSC is obviously higher than all other baseline methods. This is due to the added adaptation layer and the shrunk output range caused by it. We provide a detailed explanation as follows.

By using the monotonicity of linear-fractional functions $Q_i(\cdot)$, we can easily compute the range of the model output. Since $g(\mathbf{x}) \in [0, 1]$, by plugging in $g(\mathbf{x}) = 0$ and $g(\mathbf{x}) = 1$ respectively we

Table 4: Means (standard deviations) of the classification error over three trials in percentage of each method on learning from 10, 25 and 50 U sets. Best and comparable methods (paired t -test at significance level 5%) are highlighted in boldface.

Dataset	Sets	MMC-unbiased	MMC-ReLU	LLP-VAT	U^m -SSC
MNIST	10	6.48(1.11)	4.88(0.78)	3.49(0.21)	2.86(0.11)
	25	6.49(0.78)	3.61(0.41)	3.82(0.22)	3.1(0.19)
	50	5.86(0.75)	3.26(0.19)	3.16(0.18)	2.89(0.1)
Fashion-MNIST	10	13.71(0.98)	10.24(1.85)	14.03(0.53)	6.2(0.33)
	25	11.66(0.56)	7.96(0.37)	16.37(0.27)	6.17(0.07)
	50	12.58(2.61)	8.16(0.63)	14.54(0.25)	6.13(0.08)
Kuzushiji-MNIST	10	18.82(3.44)	14.3(3.04)	19.66(0.33)	9.58(0.23)
	25	14.58(1.33)	10.96(0.91)	11.92(0.23)	8.89(0.51)
	50	15.53(0.54)	11.61(0.51)	20.08(0.35)	9.41(0.88)
CIFAR-10	10	18.05(1.25)	17.05(0.41)	17.58(3.75)	13.64(0.11)
	25	16.78(1.61)	15.59(0.65)	14.16(0.8)	13.33(0.11)
	50	17.25(0.97)	15.8(0.96)	15.02(0.56)	13.31(0.29)

get

$$Q_i(0) = \frac{b_i}{d} = \frac{\rho_i \pi_{\mathcal{D}}(1 - \pi_i)}{\sum_{j=1}^m \rho_j \pi_{\mathcal{D}}(1 - \pi_j)},$$

$$Q_i(1) = \frac{a_i + b_i}{c_i + d} = \frac{\rho_i \pi_j(1 - \pi_{\mathcal{D}})}{\sum_{j=1}^m \rho_j \pi_j(1 - \pi_{\mathcal{D}})}.$$

According to our generation processes of class priors and set size, $\pi_i \in [0.1, 0.9]$ and $\rho_i = 1/m$ for any $i = 1, \dots, m$. Thus the upper bound of model output: $\max(Q_i(0), Q_i(1))$ takes its value around 0.1 to 0.01. As the result, the cross-entropy gives the loss in range [2.3, 4.6], which is relatively high than usual training loss, e.g., three baseline methods.

The effect of high training loss appears in hyper-parameters tuning especially for learning rate. We need to choose a relatively small learning rate, e.g., searching learning rate from $\{10^{-6}, 10^{-5}, 10^{-4}\}$ to maximize the performance.

C.3 Robustness against Inaccurate Class Priors

Table 5 reports the test performance of each method on learning from inaccurate class priors.

C.4 On the Variation of Set Numbers Results

Another main factor that potentially affects the performance of the proposed method is the number of available U sets. As U data can be easily collected from multiple resources, the learning algorithm is desired to possess the ability to handle a different number of U sets. The experimental results

Table 5: Means (standard deviations) of the classification error over three trials in percentage for the U^m -SSC method tested on inaccurate class priors.

Dataset	Sets	True	$\epsilon = 0.1$	$\epsilon = 0.2$	$\epsilon = 0.4$
MNIST	10	2.95(0.07)	3.17(0.07)	3.56(0.11)	3.75(0.03)
	50	2.86(0.11)	2.76(0.1)	3.19(0.15)	3.42(0.06)
Fashion-MNIST	10	8.32(0.24)	8.08(0.18)	8.16(0.27)	8.37(0.55)
	50	7.65(0.25)	7.77(0.07)	7.99(0.24)	7.35(0.21)
Kuzushiji-MNIST	10	9.73(0.48)	8.87(0.13)	8.77(0.17)	9.3(0.21)
	50	8.49(0.24)	8.75(0.21)	8.75(0.29)	8.58(0.41)
CIFAR-10	10	13.17(0.32)	12.72(0.43)	13.42(0.46)	13.39(1.24)
	50	12.67(0.14)	12.82(0.4)	13.68(0.42)	14.28(0.29)

Table 6: Means (standard deviations) of the classification error over three trials in percentage for the U^m -SSC method tested on different set size.

Dataset	2 U sets	100 U sets	500 U sets	1000 U sets
MNIST	2.36(0.27)	2.59(0.11)	3.07(0.14)	2.84(0.16)
Fashion-MNIST	7.95(0.85)	8.61(0.43)	8.5(0.44)	8.64(0.26)
Kuzushiji-MNIST	9.68(0.96)	10.2(0.5)	11.64(0.54)	10.68(0.4)
CIFAR-10	13.21(1.26)	13.3(0.65)	12.98(0.37)	13.16(0.7)

of learning from 10, 25, and 50 U sets have already been shown in section 5.2. But cases for extremely small number ($m = 2$) or large number ($m=1000$) should be considered and tested. Thus we conducted extensive experiments for U^m -SSC on different numbers of U sets. The final test results of learning from 2, 100, 500, and 1000 U sets are recorded in Table 6. To compare the performance change more intuitively, the CER curve on 4 benchmark datasets is shown in Figure 5.

From the results, a lower classification error can be observed for learning from 2 U sets across all 4 datasets. We conjecture the better performance is due to the large number ($T/2$) of data in a single set. Since our method connects two posterior probabilities under the distribution assumption of U marginal densities, an increasing number of sampled instances guarantee a better approximation of corresponding density distribution according to the law of large numbers. Despite the specific superiority of learning from 2 U sets, we also find a very steady performance of the proposed method against the change in the number of U sets. Combine with verified robustness of different set sizes, we conclude that U^m -SSC is practical and can easily be applied in all kinds of combinations between set size set numbers.

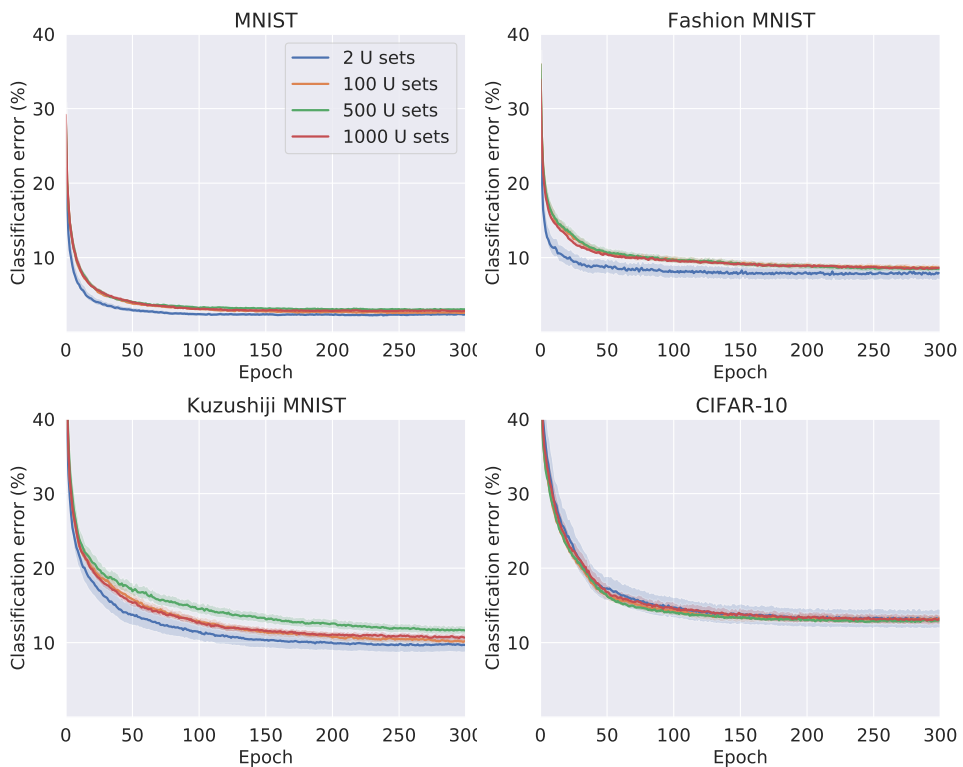


Figure 5: Experimental results of learning from different number of U sets